

NAS 12-2081

July 1969

N70-11656

NASA CR-8627



MASSACHUSETTS INSTITUTE OF TECHNOLOGY

RE-62

Optimum Mixing of Inertial Navigator and Position Fix Data

by

Walter M. Hollister* & Michel Claude Brayard†

**CASE FILE
COPY**

MEASUREMENT SYSTEMS LABORATORY

MASSACHUSETTS INSTITUTE OF TECHNOLOGY
CAMBRIDGE 39, MASSACHUSETTS

RE-62

Optimum Mixing of Inertial Navigator and Position Fix Data

by

Walter M. Hollister* & Michel Claude Brayard†

August 1969

RE-62

Optimum Mixing of Inertial Navigator and Position Fix Data

by

Walter M. Hollister* & Michel Claude Brayard†

August 1969

Approved:

W. Marchay

Director
Measurement Systems Laboratory

*Associate Professor, Massachusetts Institute of Technology

†Dupont Fellow, now Staff Engineer, M.I.T., Instrumentation Lab.

ACKNOWLEDGEMENT

This research was carried out under National Aeronautics and Space Administration Electronics Research Center Contract No. NAS 12-2081 with the Measurement Systems Laboratory, Massachusetts Institute of Technology, Cambridge, Massachusetts.

The publication of this report does not constitute approval of the findings or conclusions by the National Aeronautics and Space Administration. Distribution is provided for the exchange and stimulation of ideas.

ABSTRACT

The filtering problem is studied analytically for a system composed of an inertial navigator giving continuous indication of position and velocity and an external position fixing device giving continuous or discrete positional information. Accelerometer and external position errors are represented by white noise. Gyro drift is represented by a random walk process. Reasonable approximations lead to simplified models plus analytic predictions of the filter's performance. The analytic results are verified by comparison with computer simulations using more accurate models. Error growth of the inertial navigator without external information is shown to be extremely small for the first eight minutes following alignment. During that interval accelerometer noise is the predominant source of error. Estimation of the platform misalignment is not necessary unless the inertial system must subsequently navigate without external position information.

NOMENCLATURE

a	= vehicle acceleration, ft/sec^2
c	= platform misalignment times earth radius, ft
d	= drift rate of gyro times earth radius, ft/sec
F	= system parameters matrix
g	= acceleration due to gravity, ft/sec^2
H	= measurement matrix
I	= identity matrix
K	= filter gain matrix
L	= latitude, rad
m	= measurement, ft
n	= accelerometer noise, ft/sec^2
N	= power spectral density of accelerometer noise, ft^2/sec^3
P	= covariance matrix
<u>q</u>	= system noise vector
Q	= power spectral density of system noise matrix
r	= position error of inertial navigator, ft
r_n	= error in the external position information, ft
R	= power spectral density of external position error, $\text{ft}^2 \text{ sec}$
R_e	= earth's radius, ft
s	= Laplace operator
t	= time, sec
v	= velocity error of inertial navigator, ft/sec
V	= variance of external position fix, ft^2
w	= white noise source for gyro drift, ft/sec
W	= power spectral density of gyro noise source, ft^2/sec^3

\underline{x}	= system state vector
α	= ratio of $1/\Delta t$ and filter natural frequency
γ^4	= ratio of gyro and accelerometer noise sources
Δt	= time interval between position fixes, sec
$\epsilon(r)$	= error in the estimate of r , ft
σ_r^2	= variance in variable, r , ft^2
ω_{ie}	= earth rate, rad/sec
ω_n	= natural frequency of filter, rad/sec
ω_s	= Schuler frequency, rad/sec

Superscripts

\cdot	= time derivative
\wedge	= estimate
T	= transpose
$-$	= before measurement
$+$	= after measurement

Subscripts

x	= north component
y	= east component
z	= vertical component

Introduction

A promising method of aircraft navigation involves the optimum mixing of inertially derived position and velocity data together with radio position fixes. The optimum filter for mixing the data requires a mathematical model of the error propagation. It is desirable that the model be as simple as practicable because of the large number of mathematical operations involved in the implementation of the filter. A simple model is also of practical necessity in order to obtain analytic expressions for the elements of the covariance matrix. The purpose of this work is to show how the filter can be simplified through valid approximations and analyzed analytically. The work is motivated by an application where position fixes are available at a rapid rate (every few seconds) for a relatively short period of time (five to ten minutes). Subsequently, the inertial system is required to navigate without external fix information. Consequently, the filter should estimate the alignment error of the inertial system in addition to current position and velocity. A practical example of this situation occurs during an instrument approach or departure where very precise position data is available. Typical specifications are a 10 ft position uncertainty and a 3 ft/sec velocity uncertainty while external information is available.

The simplifications which result are valid when the time between fixes is less than one tenth of a Schuler period. A computer simulation was used to verify the predicted range of validity by comparing the approximate models against more accurate models. The results have proven to be generally applicable to situations

where the inertial system is updated at an interval less than one tenth the Schuler period. Theory would predict a significant loss of accuracy if the system were updated at any slower rate. Consequently, the analysis should be applicable to most cases of practical interest.

Models of the System

A block diagram of the system is shown in Figure 1. The measurement is the difference between the position given by the inertial navigator and the external fix. It is, therefore, a measure of the error in the inertial indication of position. Filtering the measurement gives an optimum estimate of all the inertial error variables. The position and velocity error estimates are subtracted from the output of the inertial system to obtain the optimum estimate of position and velocity. This approach permits the use of a linear error model for the inertial navigator. The state equation with no error sources is

$$\dot{\underline{x}} = \underline{F}\underline{x} \quad (1)$$

For a local-level, Schuler-tuned platform aligned to true north, let

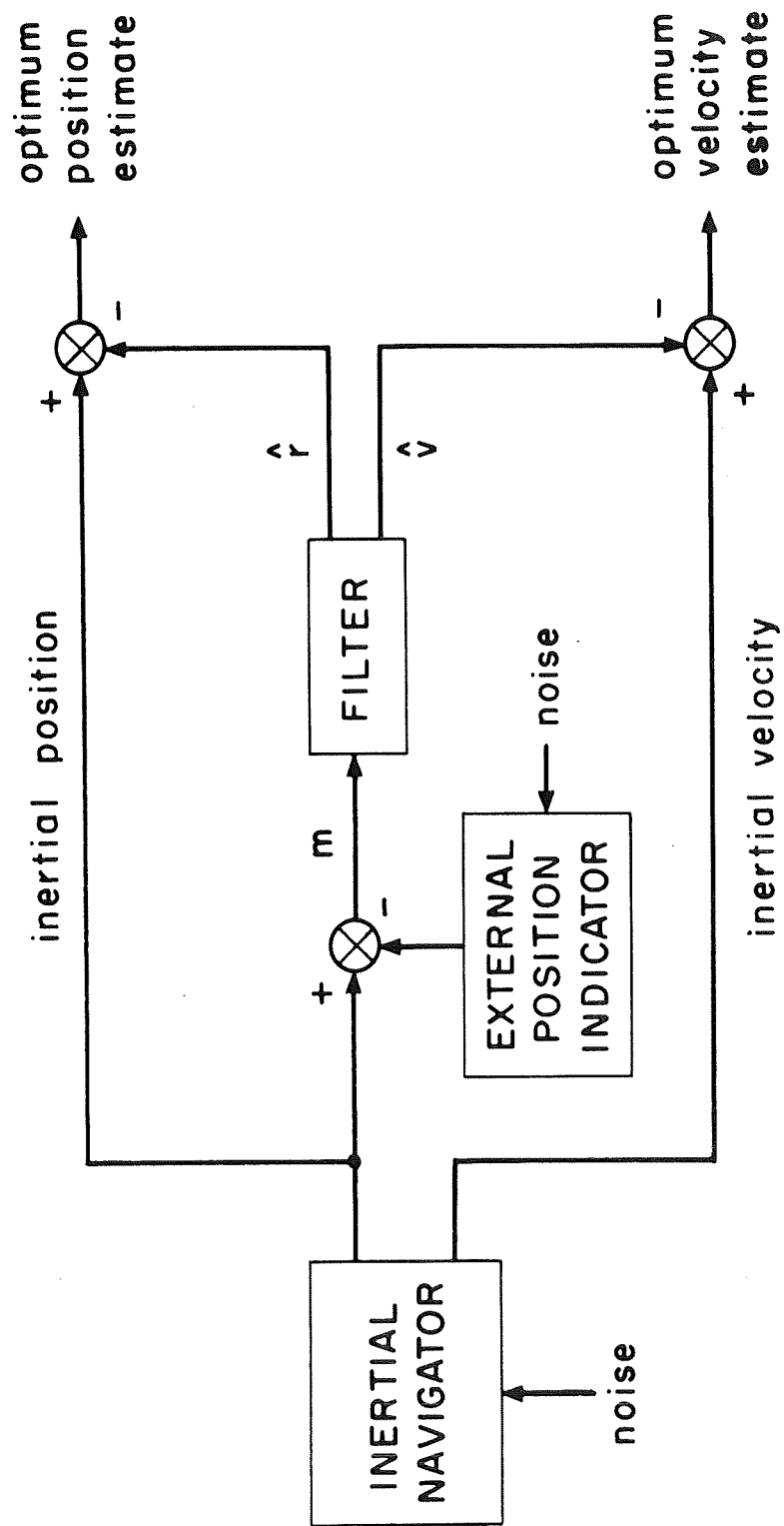


Fig. 1 Block diagram of the hybrid navigator.

$$\underline{x} = \begin{bmatrix} r_x \\ r_y \\ v_x \\ v_y \\ c_x \\ c_y \\ c_z \end{bmatrix} \quad F = \begin{bmatrix} 0 & 0 & 1 & 0 & 0 & 0 & 0 \\ 0 & 0 & 0 & 1 & 0 & 0 & 0 \\ 0 & 0 & 0 & 0 & 0 & \omega_s^2 & 0 \\ 0 & 0 & 0 & 0 & -\omega_s^2 & 0 & 0 \\ -\omega_{ie}\sin L & 0 & 0 & 1 & 0 & -\omega_{ie}\sin L & 0 \\ 0 & 0 & -1 & 0 & \omega_{ie}\sin L & 0 & \omega_{ie}\cos L \\ -\omega_{ie}\cos L & 0 & 0 & -\tan L & 0 & -\omega_{ie}\cos L & 0 \end{bmatrix} \quad (2)$$

The state, \underline{x} , represents the errors in the inertial system. The platform misalignment angles, c , are scaled by earth's radius, R_e , to give them the units in feet. The Schuler frequency, ω_s , is defined by

$$\omega_s^2 = g/R_e \quad (3)$$

The inertial error at the output of the accelerometers due to the platform misalignment is thus $\omega_s^2 c$. The choice of units is primarily for convenience. The model assumes that the vehicle velocity is small compared to $R_e \omega_{ie}$, vehicle acceleration is small in comparison to g , Coriolis accelerations are negligible, and the system does not operate close to the earth's polar axis.

Equation (1) has been solved in general for the above case.¹ From the solution it can be argued that the terms involving earth rate, ω_{ie} , have little influence on the variables for operating times of interest here. By neglecting them, the error model uncouples into two identical, Schuler-tuned, level loops. For this case

$$\underline{x} = \begin{bmatrix} r \\ v \\ c \end{bmatrix} \quad F = \begin{bmatrix} 0 & 1 & 0 \\ 0 & 0 & \omega_s^2 \\ 0 & -1 & 0 \end{bmatrix} \quad (4)$$

The model described by (4) is used as the starting point for the analytic approximation. The model described by (2) was programmed for the computer verification of the theory.

The main sources of error in the inertial system are the gyro drift and accelerometer noise. Only the random components of these errors are significant because the constant components are estimated by the filter. The random component of the gyro drift, d , is well approximated by a random walk,^(2, 3) i.e. the output of an integrator driven by a white noise, w . The random component of the accelerometer noise is approximated by a white noise, n . This is equivalent to assuming that the mean squared uncertainty in the drift rate and the mean squared uncertainty in the velocity error due to accelerometer noise both grow linearly with time. The state vector of the system must be augmented to include the random walk. The system is now described by

$$\dot{\underline{x}} = F\underline{x} + \underline{q} \quad (5)$$

where

$$\underline{x} = \begin{bmatrix} r \\ v \\ c \\ d \end{bmatrix} \quad F = \begin{bmatrix} 0 & 1 & 0 & 0 \\ 0 & 0 & \omega_s^2 & 0 \\ 0 & -1 & 0 & 1 \\ 0 & 0 & 0 & 0 \end{bmatrix} \quad \underline{q} = \begin{bmatrix} 0 \\ n \\ 0 \\ w \end{bmatrix} \quad (6)$$

Equation (5) is shown as a signal-flow diagram in Figure 2.

The error in the external position fixing device is approximated by a white noise source, r_n . This does not account for bias

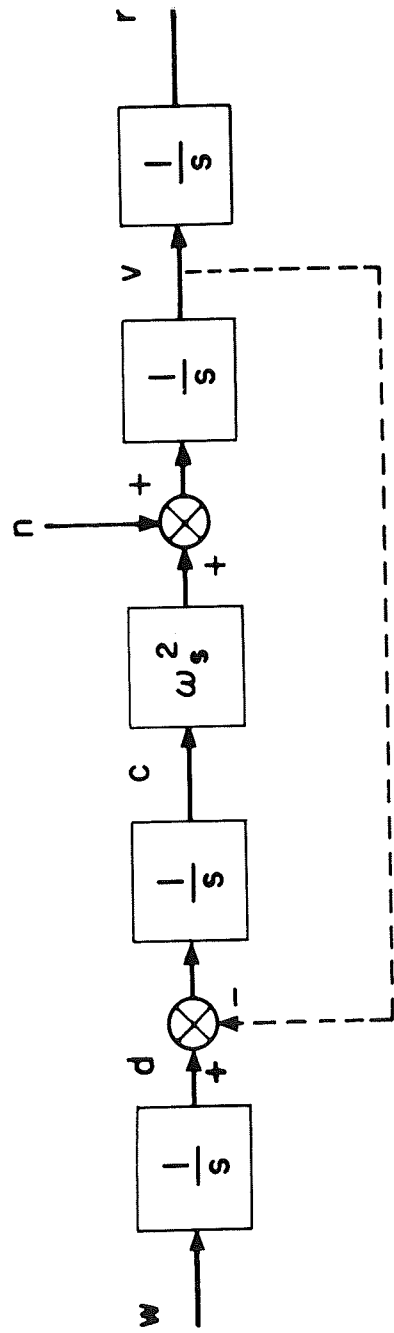


Fig.2 Error model for the inertial navigator.

or scale factor errors in the position fix.

Filtering Theory

The analytic analysis is based on the minimum variance estimator as derived by Kalman and Bucy.⁴ The system is described by (5). The measurement is given by

$$\underline{m} = H\underline{x} + r_n \quad (7)$$

The estimate is propagated by

$$\hat{\underline{x}} = F\hat{\underline{x}} + PH^TR^{-1}(\underline{m} - H\underline{x}) \quad (8)$$

The covariance matrix is propagated by

$$\dot{P} = FP + PF^T + Q - PH^TR^{-1}HP \quad (9)$$

With no measurements the estimate and the covariance matrix propagate as if R^{-1} were zero. When measurements are taken at discrete times, the same is true between measurements. The discrete measurement is contaminated by an independent, random variable with zero mean and variance, V . At each measurement the new estimate is given by

$$\hat{\underline{x}} = K \underline{m} \quad (10)$$

where

$$K = P^T H^T [HP^T H^T + V]^{-1} \quad (11)$$

$$P^+ = [I - KH] P^- \quad (12)$$

+ denotes just after the measurement and

- denotes just before the measurement

Error Propagation

Let \underline{x} and F be defined by (6). Propagate the covariance matrix when no measurements are taken by integrating (9) with R^{-1} set equal to zero. This is a set of ten coupled, linear, differential equations. These have been integrated assuming $P(0) = 0$. The result shows how the position and velocity uncertainties grow after initial alignment because of gyro drift and accelerometer noise.

$$\begin{aligned} \sigma_r^2 = & \frac{N}{\omega_s^3} \left[\frac{\omega_{st}}{2} - \frac{1}{4} \sin 2\omega_{st} \right] \\ & + \frac{W}{\omega_s^3} \left[\frac{\omega_{st}}{2} + \frac{(\omega_{st})^3}{3} - 2\sin \omega_{st} + 2\omega_{st} \cos \omega_{st} - \frac{1}{4} \sin 2\omega_{st} \right] \end{aligned} \quad (13)$$

$$\begin{aligned} \sigma_v^2 = & \frac{N}{\omega_s} \left[\frac{\omega_{st}}{2} + \frac{1}{4} \sin 2\omega_{st} \right] \\ & + \frac{W}{\omega_s} \left[\frac{3}{2} \omega_{st} + \frac{1}{4} \sin 2\omega_{st} - 2\sin \omega_{st} \right] \end{aligned} \quad (14)$$

For t small in comparison to the Schuler period, $\frac{2\pi}{\omega_s}$, these are approximated to first order by

$$\sigma_r^2 \approx \frac{N}{\omega_s^3} \frac{(\omega_{st})^3}{3} + \frac{W}{\omega_s^3} \frac{(\omega_{st})^7}{252} \quad (15)$$

$$\sigma_v^2 \approx \frac{N}{\omega_s} \omega_{st} + \frac{W}{\omega_s^3} \frac{(\omega_{st})^5}{20} \quad (16)$$

Equations (15) and (16) are the result of the integration when the system is represented by

$$F = \begin{bmatrix} 0 & 1 & 0 & 0 \\ 0 & 0 & \omega_S^2 & 0 \\ 0 & 0 & 0 & 1 \\ 0 & 0 & 0 & 0 \end{bmatrix} \quad (17)$$

as can be verified by solving a simpler set of ten linear, differential equations. The signal flow diagram for the system represented by (17) is the same as that shown in Figure 2, but with the dotted feedback path removed. The units of N and W are identical. Let

$$\frac{W}{N} = \gamma^4 \quad (18)$$

Equations (13) - (16) are plotted in Figures 3-7 for $\gamma = 4$. Over long time intervals the position uncertainty is dominated by the contribution due to gyro drift. For very short time intervals, however, the greater contribution to the uncertainty comes from the accelerometer noise. For $\omega_S t < 1$, the two contributions are equal when

$$\frac{1}{3} N t^3 = \gamma^4 \omega_S^4 N \frac{t^7}{252} \quad (19)$$

$$\gamma \omega_S t \cong 3.0$$

$$\text{For } \gamma = 4 \quad t \cong 10 \text{ min}$$

The fundamental conclusion from this analysis is that the position uncertainty of an aligned inertial system remains relatively small for the first tenth of a Schuler period. During that time the major error source is the accelerometer noise. After that time the gyro drift takes over and the uncertainty grows rapidly. The theory

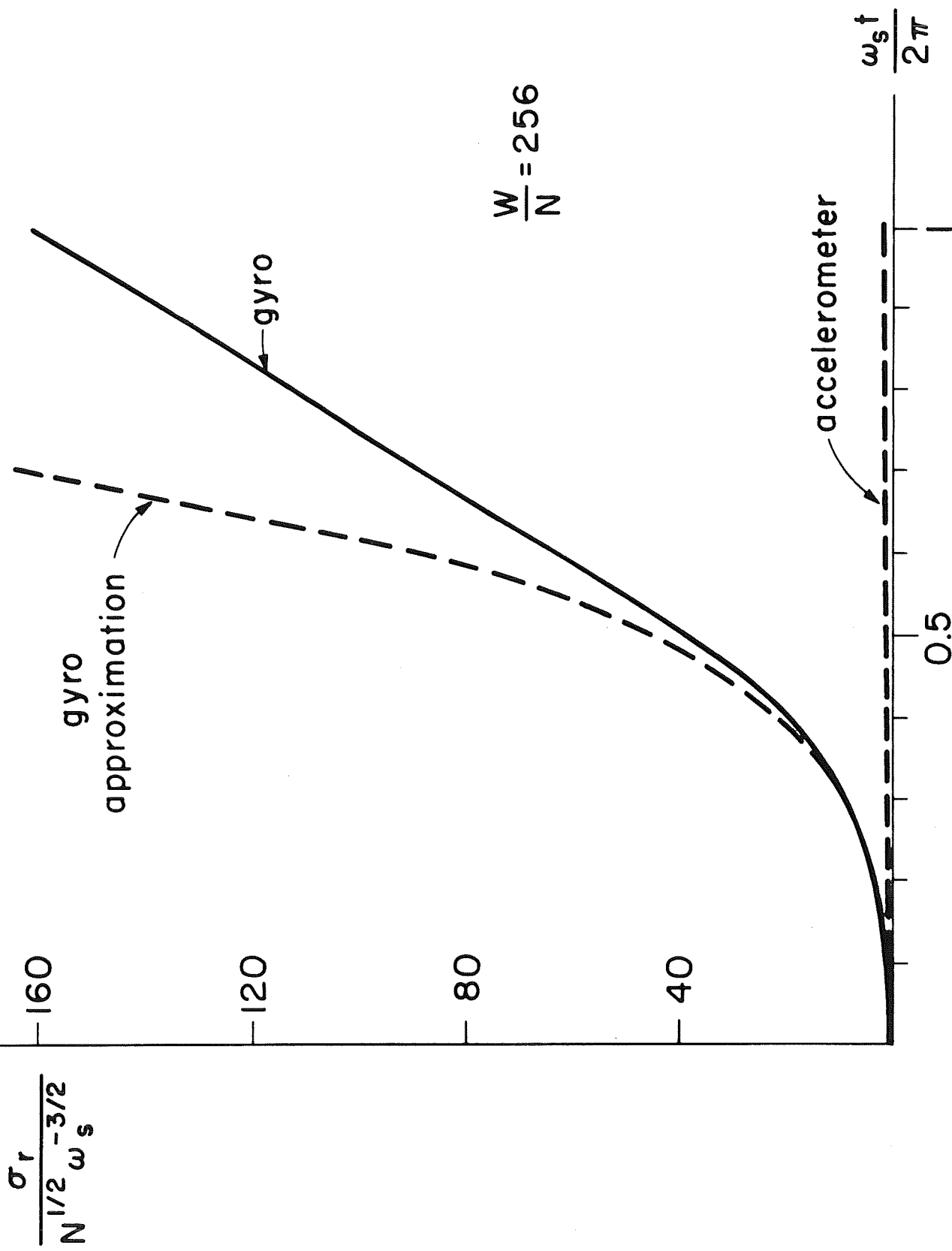


Fig.3 Position uncertainty due to gyro drift.

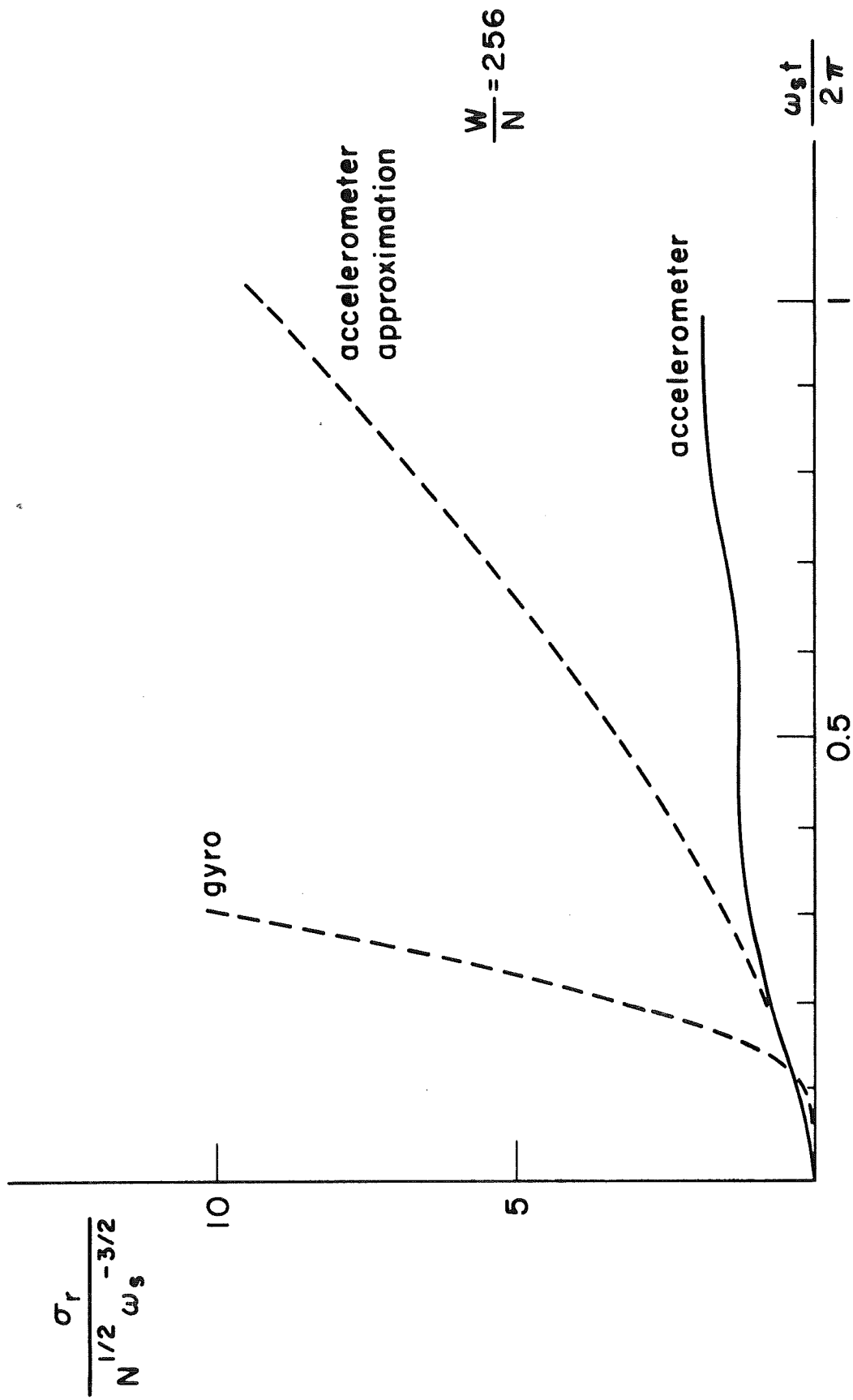


Fig. 4 Position uncertainty due to accelerometer noise.

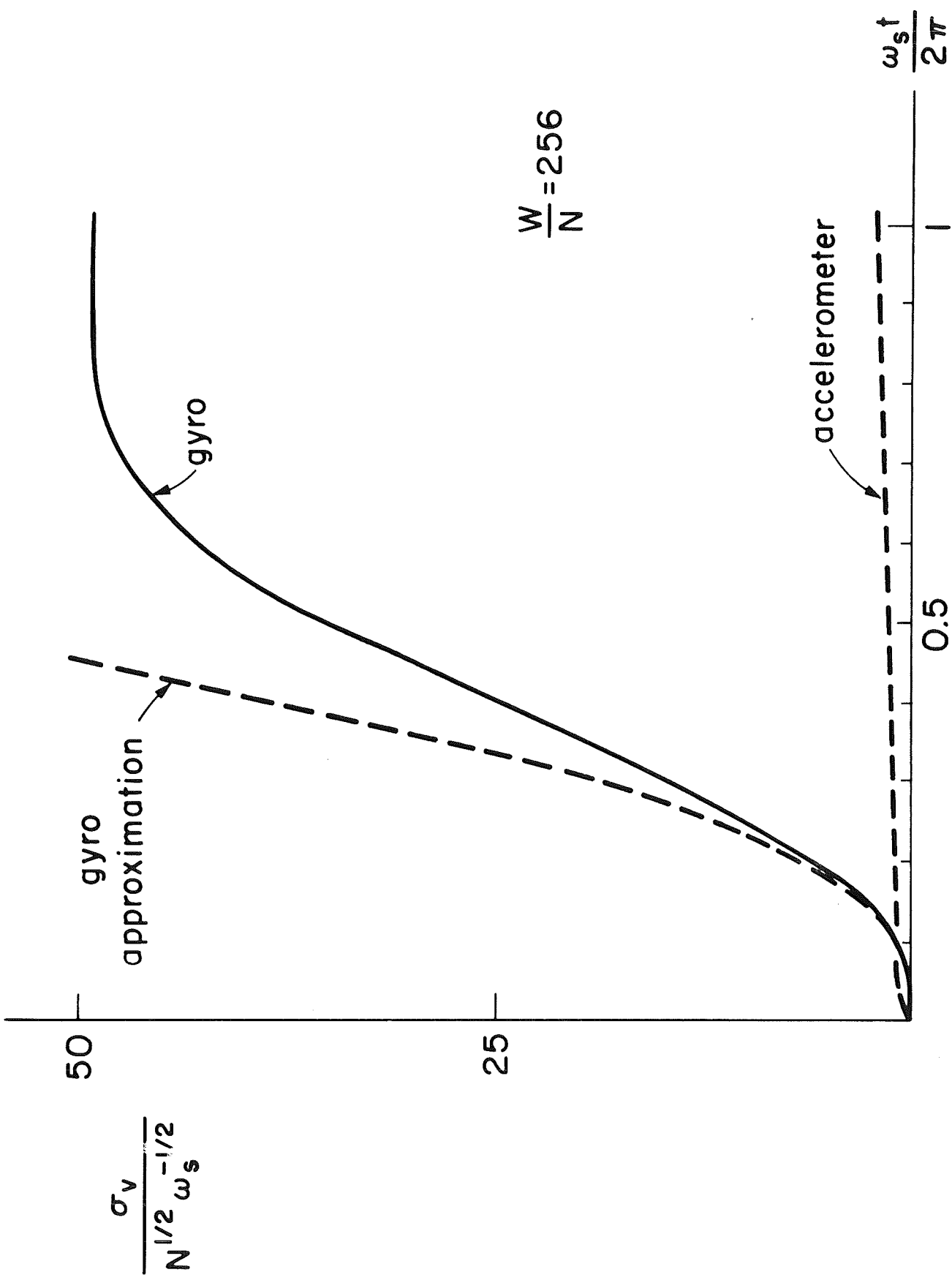


Fig.5 Velocity uncertainty due to gyro drift.

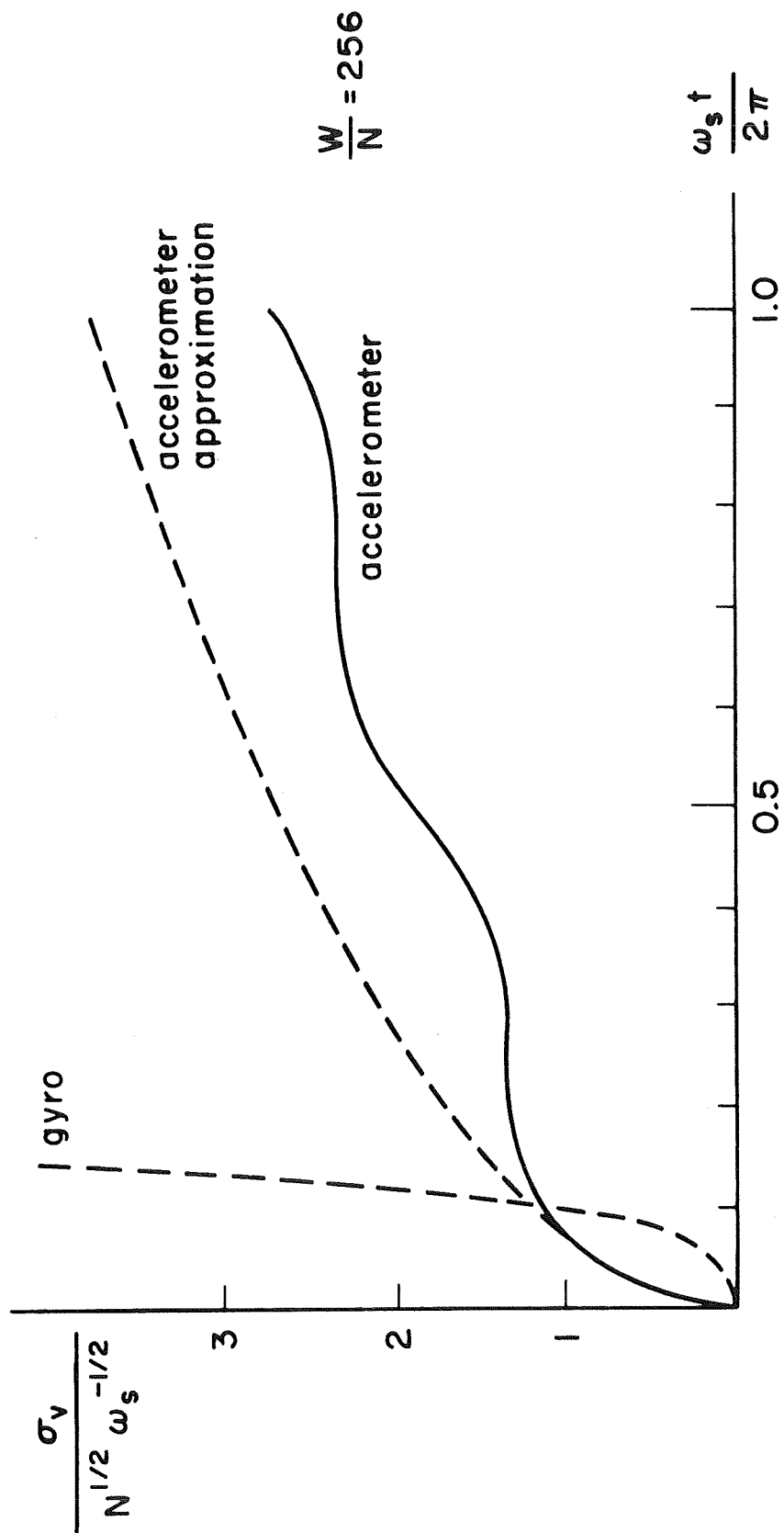


Fig.6 Velocity uncertainty due to accelerometer noise.

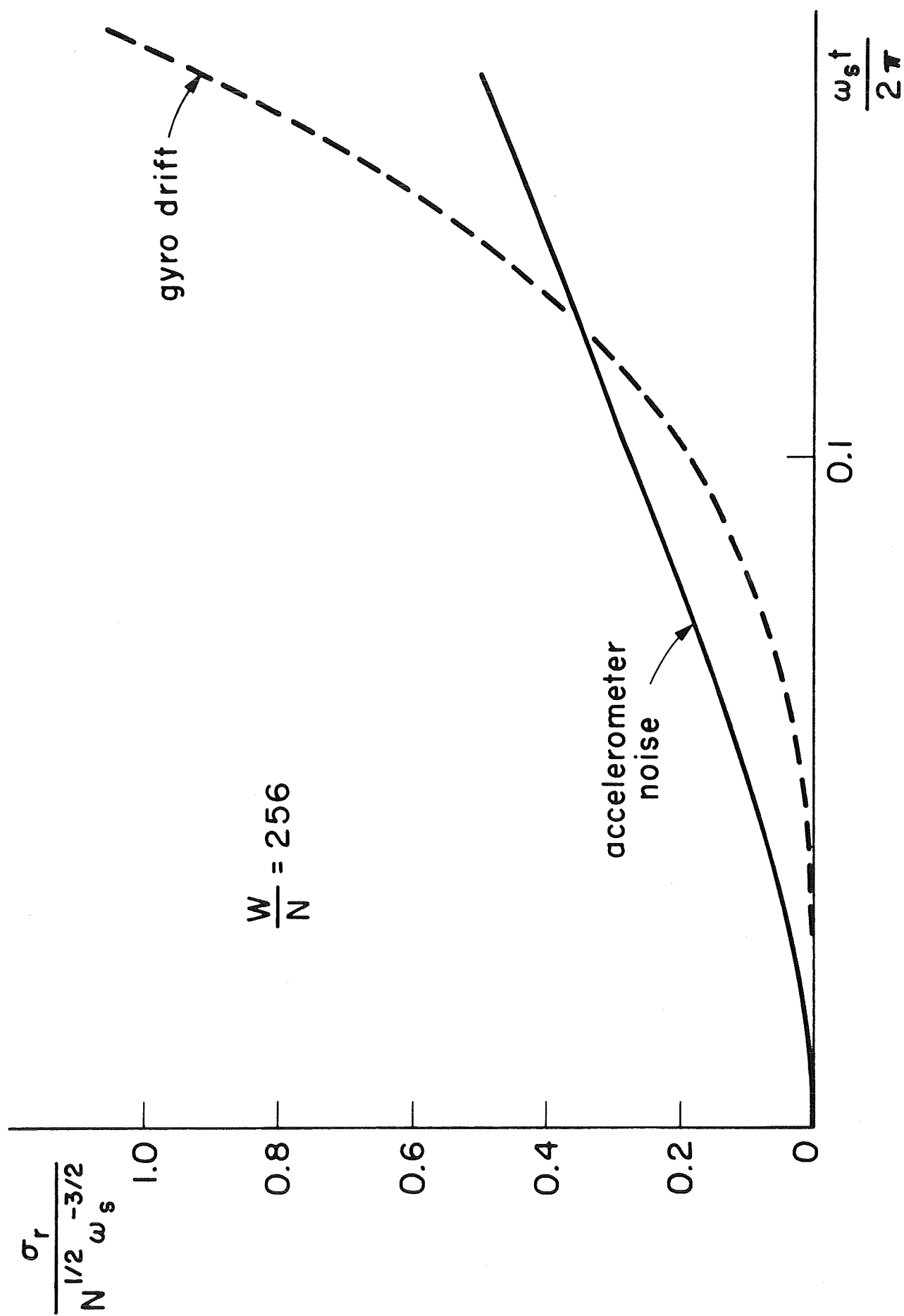


Fig.7 Position uncertainty just after alignment.

predicts very small position uncertainty if the system can be re-aligned at intervals less than one tenth Schuler period. The conclusion is supported by the observation of actual inertial navigator data.⁽⁵⁾

Continuous Filtering

The analysis of the previous section has shown that for short time periods, the position uncertainty is dominated by the accelerometer noise, and the accelerometer noise propagation is well approximated by two simple integrations. Since the gyro drift, d , and platform misalignment, c , have a negligible effect on the position and velocity uncertainty, they are temporarily dropped from the state, \underline{x} .

$$\underline{x} = \begin{bmatrix} r \\ v \end{bmatrix} \quad F = \begin{bmatrix} 0 & 1 \\ 0 & 0 \end{bmatrix} \quad \underline{q} = \begin{bmatrix} 0 \\ n \end{bmatrix} \quad (20)$$

The filter equations describing this simple system have been completely solved by Potter and VanderVelde.⁽⁶⁾ The steady-state solution gives

$$\sigma_r^2 = \sqrt{2} \ N^{1/4} \ R^{3/4} \quad (21)$$

$$\sigma_v^2 = \sqrt{2} \ N^{3/4} \ R^{1/4}$$

$$\text{Define} \quad \omega_n^4 = \frac{N}{R} \quad (22)$$

The steady-state filter gain is

$$K = \begin{bmatrix} \sqrt{2} & \omega_n \\ & \omega_n^2 \end{bmatrix} \quad (23)$$

The transient behavior of the filter gain depends on the initial value of P , but it is within a few percent of the steady state value after $\omega_n t > 2$. Consequently, $\frac{2}{\omega_n}$ is a prediction of the time to reach steady state. The filter is shown in Figure 8. The error in the estimate of inertial position error is related to the actual inertial position error by

$$\frac{\varepsilon(\hat{\mathbf{r}})}{\mathbf{r}} = \frac{s^2}{s^2 + \sqrt{2} \omega_n s + \omega_n^2} \quad (24)$$

Only that part of the inertial error with frequency component at or above ω_n fails to be estimated correctly by the filter. Components of error at the Schuler frequency, for example, are attenuated by the factor $\left(\frac{\omega_s}{\omega_n}\right)^2$. It can be shown that the filter which includes the Schuler loop as represented by Equation (4) reduces to the simple filter above so long as $\omega_s \ll \omega_n$.

Next, model the inertial system by the state equations given by (17) so that the misalignment angle and the drift can be estimated. This model is a good approximation of the error propagation over short intervals and is simple enough so that the filter can probably be determined analytically using the method described in reference (6). Attention is focused on the steady-state solution which for $\gamma\omega_s < \omega_n$ is given approximately by

$$\begin{aligned} \sigma_r^2 &= \sqrt{2} N^{1/4} R^{3/4} \\ \sigma_v^2 &= \sqrt{2} N^{3/4} R^{1/4} \\ \sigma_c^2 &= \sqrt{2} W^{1/4} \left(\frac{N}{\omega_s^4}\right)^{3/4} \\ \sigma_d^2 &= \sqrt{2} W^{3/4} \left(\frac{N}{\omega_s^4}\right)^{1/4} \end{aligned} \quad (25)$$

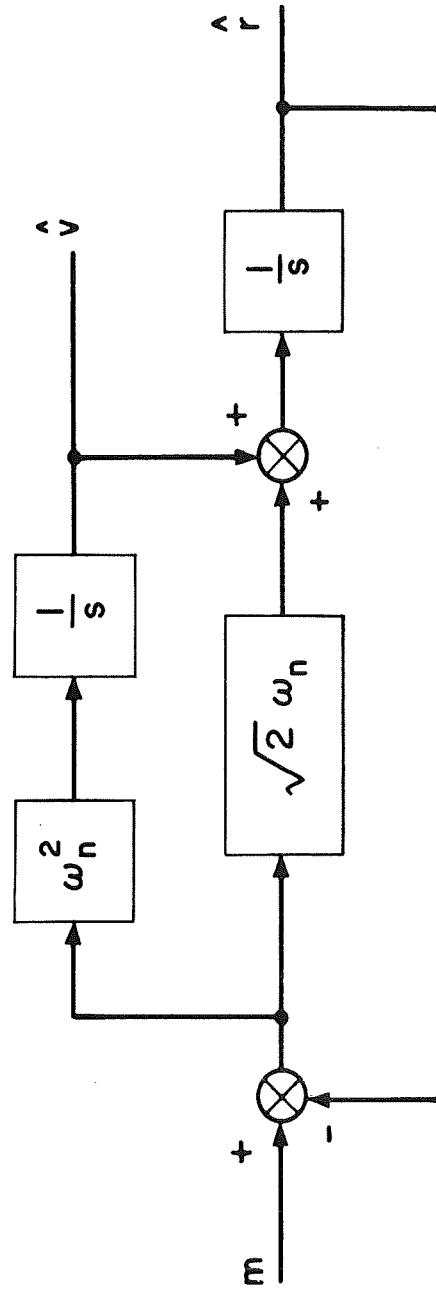


Fig. 8 Optimum steady-state filter for position and velocity errors.

To a first order approximation the position and velocity uncertainty are the same as they were when the drift and misalignment were not estimated.

The accuracy of the misalignment and drift estimates are determined by the gyro drift and accelerometer noise alone. The same accuracy would result if c and d were optimally estimated by looking at the output of the accelerometer with the vehicle at rest and with no input to the gyro other than the drift itself. This is just the process which takes place during ground alignment. Note that estimation of misalignment by the filter and physical alignment of the system are equivalent so long as the model used by the filter is a satisfactory representation of the physical system. Therefore, under the assumption, $\gamma\omega_s < \omega_n$, the inflight estimate of drift and misalignment can be as accurate in the steady state as a ground alignment. The steady-state filter gain is given by

$$K \cong \begin{bmatrix} \sqrt{2} \omega_n \\ \omega_n^2 \\ \sqrt{2} \gamma \frac{\omega_n^2}{\omega_s} \\ \gamma^2 \omega_n^2 \end{bmatrix} \quad (26)$$

The filter is shown in Figure 9. For this filter the error in the estimate of inertial position error is related to the actual inertial error by

$$\frac{\hat{\epsilon}(\mathbf{r})}{r} \cong \frac{s^4}{(s^2 + \sqrt{2} \omega_n s + \omega_n^2)(s^2 + \sqrt{2} \gamma \omega_s s + \gamma^2 \omega_s^2)} \quad (27)$$

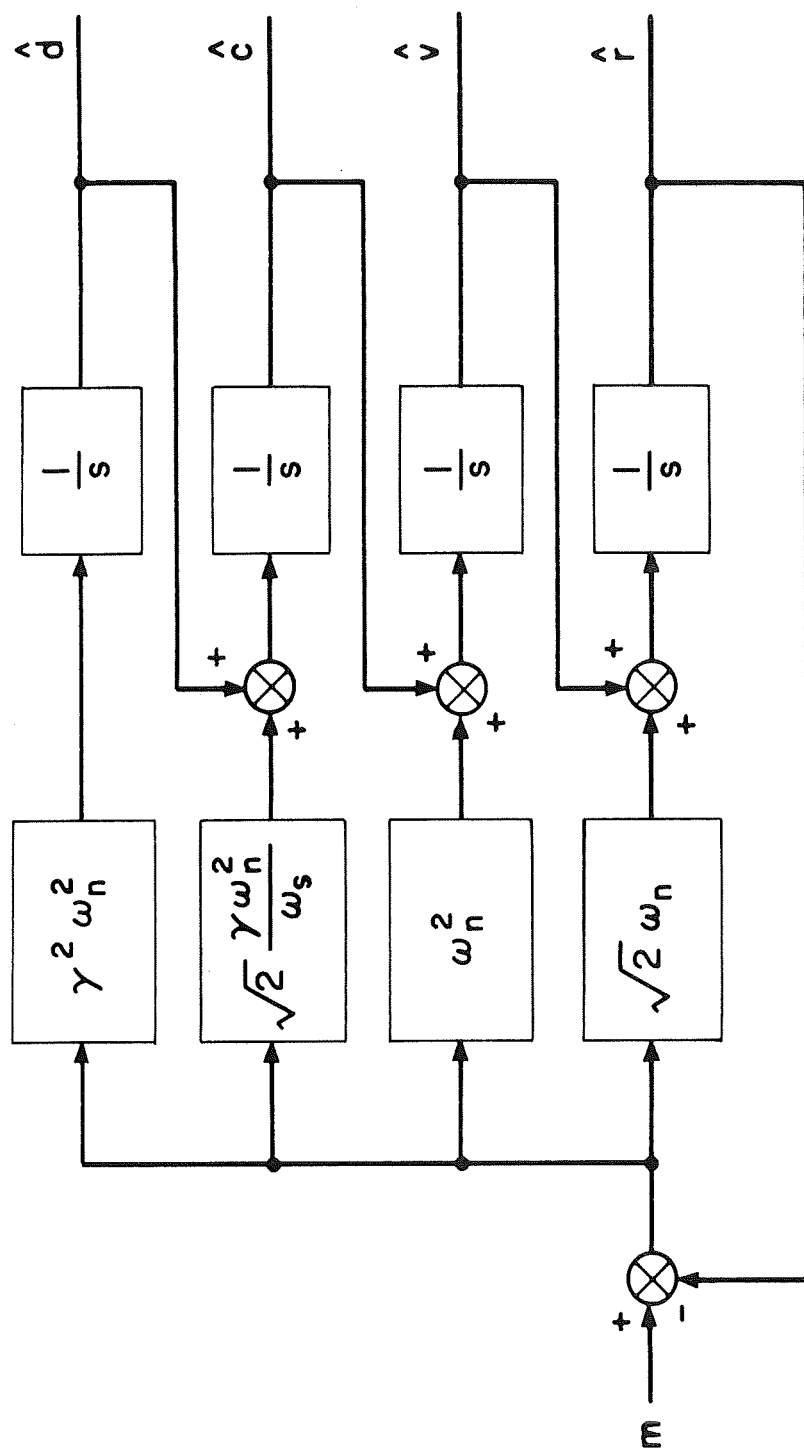


Fig.9 Steady-state filter for position, velocity, misalignment and drift.

Equation (27) is plotted in Figure 10. It can be seen that the estimation of the drift and the misalignment do not appreciably affect the steady-state position error because the more complex filter only decreases frequency components which were already heavily attenuated. It is expected that $2/\omega_n$ is a measure of the estimation time for position and velocity while $2/\gamma\omega_s$ is a measure of the estimation time for misalignment and drift. To verify this it is necessary to integrate (9) for the transient values of the covariance matrix.

Discrete Filtering

It is possible to relate any discrete filtering problem to what will be called its "continuous approximation," provided the time between measurements, Δt , is not too large. The connection is made by assuming

$$R = V \Delta t \quad (28)$$

This can be understood by deriving the continuous case variance equation from the discrete case scheme. For short time intervals, Δt , the covariance matrix can be expanded in a Taylor series

$$\begin{aligned} P(t_n)^- &= P(t_{n-1}) + F(t_{n-1}) P(t_{n-1}) \Delta t \\ &+ P(t_{n-1}) F^T(t_{n-1}) \Delta t + Q\Delta t + \text{higher order terms} \end{aligned} \quad (29)$$

At the measurement time update $P(t_n)^-$

$$P(t_n)^+ = P(t_n)^- - P(t_n)^- H^T \left[H P(t_n)^- H^T + \frac{R}{\Delta t} \right]^{-1} H P(t_n)^- \quad (30)$$

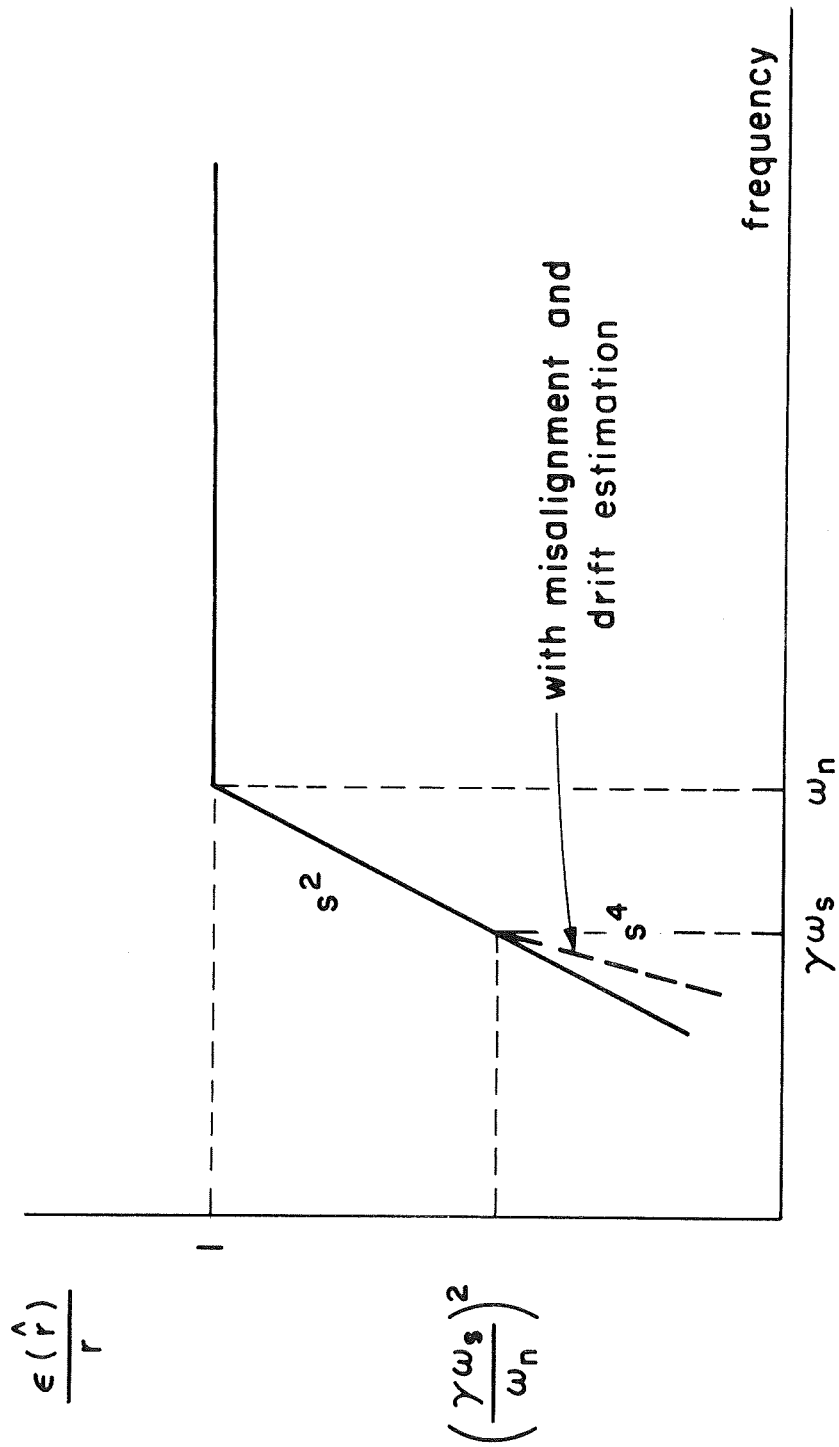


Fig. 10 Frequency response of the error in position estimate to actual inertial error.

This yields finally

$$\begin{aligned} \frac{P(t_n)^+ - P(t_{n-1})}{\Delta t} &= F(t_{n-1}) P(t_{n-1}) + P(t_{n-1}) F^T(t_{n-1}) \\ &+ Q - P(t_n)^- H^T [HP(t_n)^- H^T \Delta t + R]^{-1} HP(t_n)^- \end{aligned} \quad (31)$$

which becomes Equation (9) in the limit as Δt approaches zero.

Now consider the limitation on the time between measurements. If the discrete process yields the same results as the continuous one, this means that the position error in the discrete process does not depend upon the model chosen to represent the inertial system (since this has been shown to be true in the continuous case). But the models were shown to be equivalent only for a duration of one tenth of a Schuler period. Therefore it seems consistent to take as one time limit for the continuous approximation the same value, one tenth of a Schuler period. In addition, the assumption of (28) implies that the impulse representing the autocorrelation function of the measurement noise can be replaced by a triangular curve of height, V , but equivalent area, R . Although these curves are not the same, they yield the same results if Δt is small in comparison to the response time of the system. In this case $1/\omega_n$ represents the characteristic time of the filter fed by the measurement noise. Therefore the continuous approximation is only valid for $\Delta t < 1/\omega_n$. The excursion of the position uncertainty between measurements as a fraction of the average steady-state position uncertainty is found from (11):

$$\frac{1}{1 + \frac{V}{\sigma_r^2}} = \frac{1}{1 + \frac{1}{\sqrt{2} \omega_n \Delta t}} = \frac{1}{1 + \frac{\alpha}{\sqrt{2}}} \quad (32)$$

$$\alpha = \frac{1}{\omega_n \Delta t} \quad (33)$$

The restriction on the validity of the continuous approximation also defines the desirable range of operation. If $\alpha < 1$, the maximum excursions of the position uncertainty during the interval between measurements will be large compared to the average value. Combining Equations (21), (22), (28) and (33) gives

$$\alpha = \frac{\sqrt{2} V}{\sigma_r^2} \quad (34)$$

The choice of α on the basis of (33) fixes the ratio of external fix accuracy to position uncertainty.

Computer Verification of Theory

The validity of the simplified models was checked by programming the computer with the more rigorous model of Equation (2) and comparing results. The details of the computation are contained in Reference 7. The results are summarized below:

1. It was found that the error propagation using the most rigorous model of the inertial system was indistinguishable from that predicted by Equations (13) and (14) when plotted to the scales of Figures 3-6.

2. For continuous filtering in the presence of accelerometer noise, the rms position and velocity errors are the same to three significant figures for all models of the inertial navigator.
3. The continuous approximation provides a good representation of the discrete filter when the time between updates is less than $1/\omega_n$ and one tenth of a Schuler period.

Figure 11 gives typical results. In the case shown, $N = 10^{-2}$ ft^2/sec^3 . The four curves are the result of discrete filtering with $V = 10^6 \text{ft}^2$. The time intervals between updates are 1 sec, 30 sec, 3 min, and 18 min. For the 1 sec, 30 sec and 3 min intervals the average is well predicted by the theory. The time to reach steady-state is well predicted by the $2/\omega_n$ rule. For the 18 min interval the average is a poor representation of the performance. The excursions between updates are large in comparison to the predicted average and the time to reach steady-state is longer than the rule would predict. This would appear to confirm the assumption that the continuous approximation is valid for times less than $1/\omega_n$ and one tenth of a Schuler period.

Application

The steady-state position and velocity uncertainties were given by

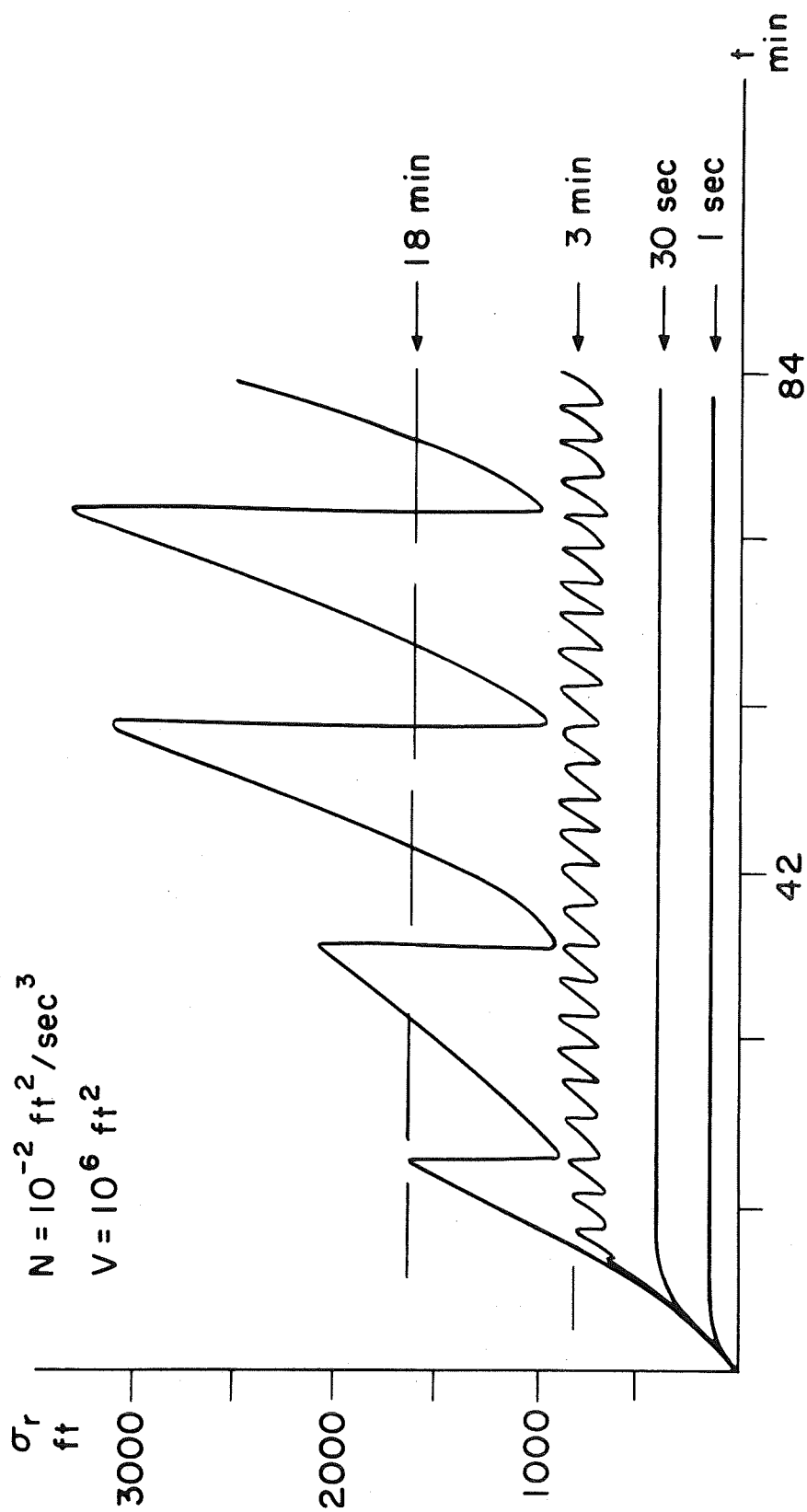


Fig. 11 Position uncertainty vs. time for different update intervals.

$$\begin{aligned}
 \sigma_r^2 &= \sqrt{2} N^{1/4} R^{3/4} = \sqrt{2} \omega_n R \\
 \sigma_v^2 &= \sqrt{2} N^{3/4} R^{1/4} = \sqrt{2} \omega_n^3 R
 \end{aligned}
 \tag{35}$$

These relationships are plotted in Figure 12. Any two variables determine the remaining three.

The steady-state misalignment and drift rate uncertainty were given by

$$\begin{aligned}
 \sigma_c^2 &= \sqrt{2} W^{1/4} \left(\frac{N}{\omega_s^4} \right)^{3/4} = \sqrt{2} \gamma \omega_s \frac{N}{\omega_s^4} \\
 \sigma_d^2 &= \sqrt{2} W^{3/4} \left(\frac{N}{\omega_s^4} \right)^{1/4} = \sqrt{2} (\gamma \omega_s)^3 \frac{N}{\omega_s^4}
 \end{aligned}
 \tag{36}$$

These relationships are plotted in Figure 13.

For discrete measurements, the continuous approximation gave average steady-state uncertainties

$$\begin{aligned}
 \sigma_r^2 &= \sqrt{2} N^{1/4} V^{3/4} \Delta t^{3/4} = \sqrt{2} N (\alpha \Delta t)^3 \\
 \sigma_v^2 &= \sqrt{2} N^{3/4} V^{1/4} \Delta t^{1/4} = \sqrt{2} N \cdot \alpha \Delta t
 \end{aligned}
 \tag{37}$$

These relationships are plotted in Figure 14.

As an example, a typical specification on position and velocity uncertainty is $\sigma_r = 10$ ft and $\sigma_v = 3$ ft/sec. The specification is met with $\omega_n = .3$ rad/sec, $N = 1.9$ ft²/sec³ and $R = 235$ ft sec. Assuming a radar with an rms position error of 15 ft, the update time should be 1.05 sec. Assuming $\gamma = 4$, the characteristics of the inertial navigator which would just meet the specification are

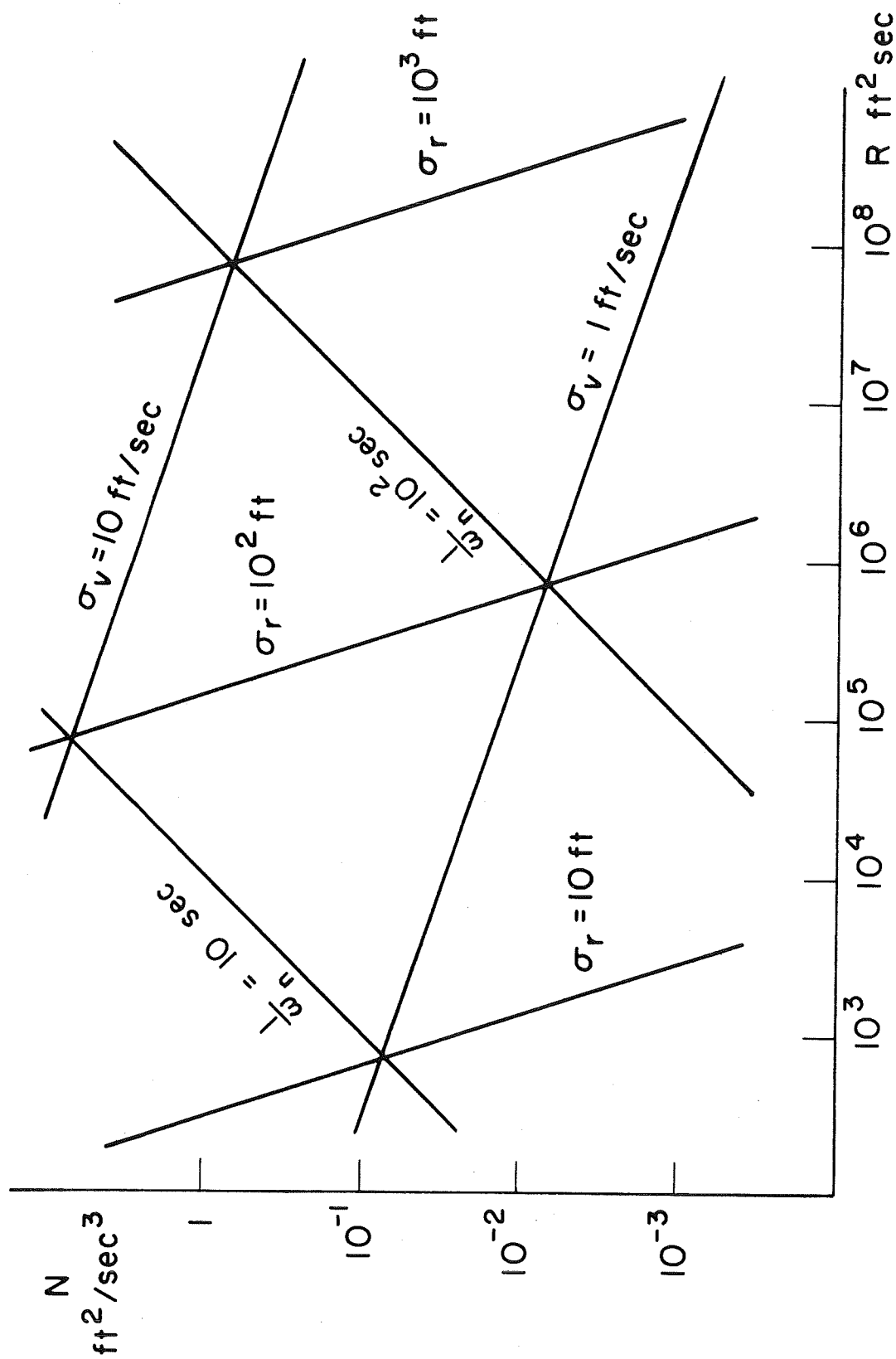


Fig.12 Position and velocity uncertainty for given error sources.

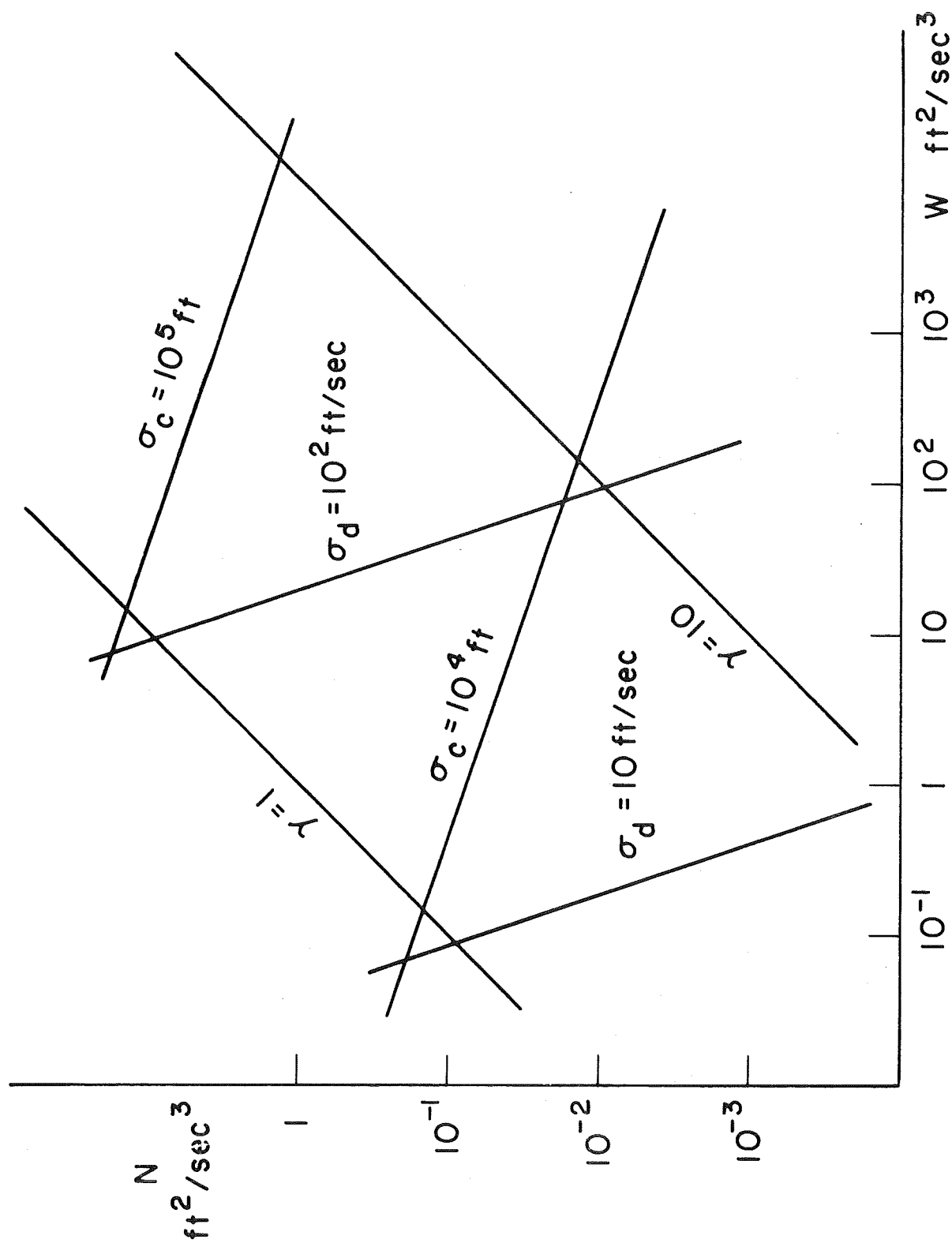


Fig. 13 Misalignment and drift uncertainty for given inertial errors.

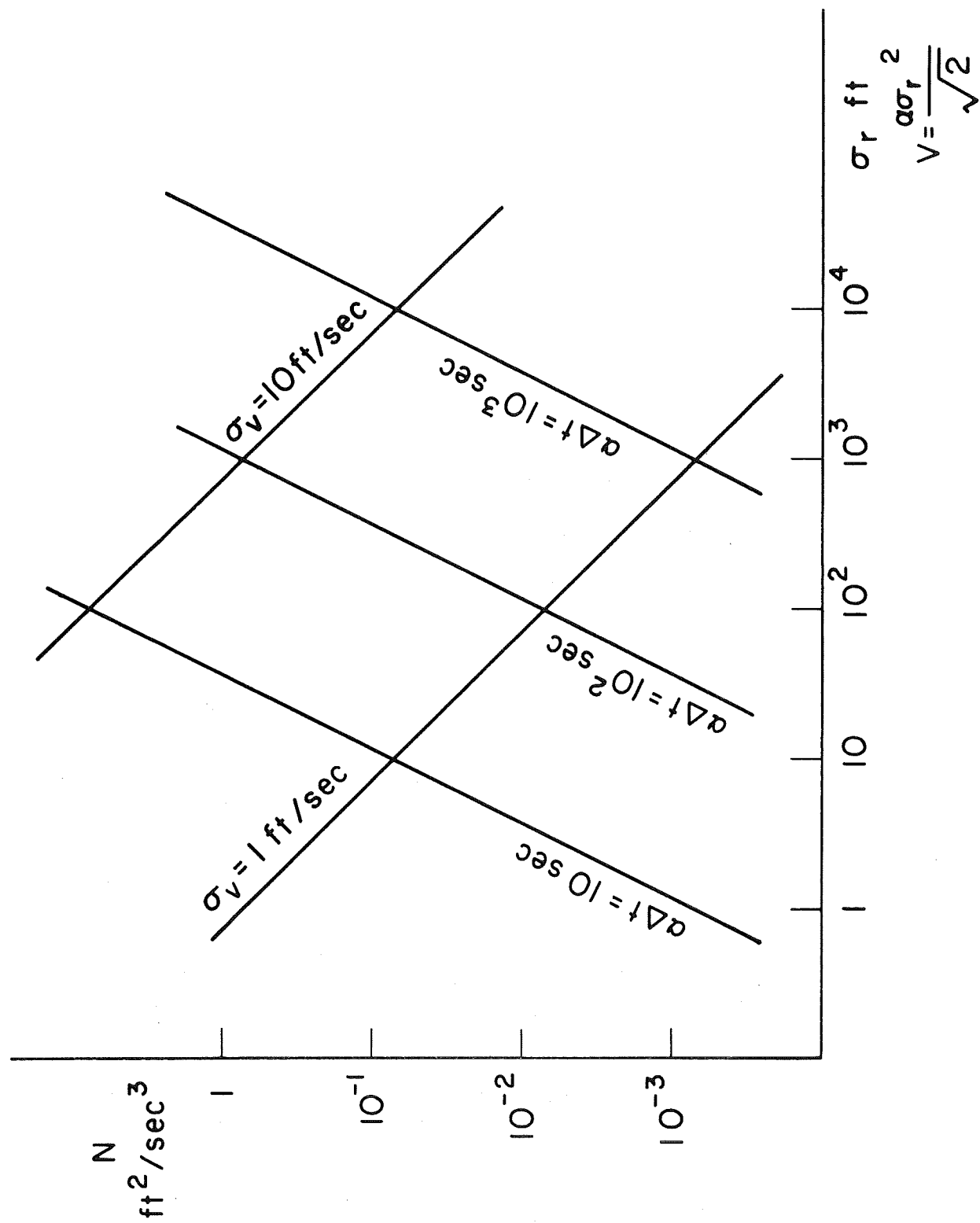


Fig.14 Position and velocity uncertainty for discrete measurements.

$$\begin{aligned}
 N &= 1.9 \text{ ft}^2/\text{sec}^3 \\
 W &= 480 \text{ ft}^2/\text{sec}^3 \\
 \sigma_c &= 74,000 \text{ ft (3.6 mrad)} \\
 \sigma_d &= 370 \text{ ft/sec}
 \end{aligned}$$

Note that the gyro drift uncertainty is over 100 times as large as the uncertainty in the estimate of velocity. For an inertial system used without update, the normal figure of merit is the velocity uncertainty which is assumed equal to the gyro drift uncertainty for long periods.

By comparison, the NASA data reported in Reference 5 can be fitted to Equation (13) giving

$$\begin{aligned}
 \gamma &= 4 \\
 N &= 3 \times 10^{-4} \text{ ft}^2/\text{sec}^3 \\
 W &= 7.68 \times 10^{-2} \text{ ft}^2/\text{sec}^3
 \end{aligned}$$

An optimum estimate of the system misalignment and drift would yield

$$\begin{aligned}
 \sigma_c &= 940 \text{ ft (.046 mrad)} \\
 \sigma_d &= 4.7 \text{ ft/sec}
 \end{aligned}$$

This system could have 75 times as much random error and still meet the previous specification, so long as external position information were available. The only need for a quality inertial system is to be able to navigate when the external information is lost.

Figure 12 shows that the accuracy of the position estimate is

dependent most upon the noise in the position measurement, while the accuracy of the velocity estimate is dependent most upon the inertial system noise. Figure 12 can also be used to predict the performance of a filter with no inertial information. The total acceleration of the vehicle would be represented by the white noise, N . The filter would estimate the total position and total velocity as opposed to their inertial errors. Such a system could give relatively good position information, but the velocity uncertainty would be large. For example, with no inertial system, the steady-state error in the position estimate due to low frequency acceleration, a , is from (24)

$$\frac{\varepsilon(\hat{r})}{a} = \frac{1}{\omega_n^2} \quad (38)$$

With an aircraft easily capable of accelerations of one half "g", ω_n would have to be raised above one rad/sec to meet the position error specification. A much better radar would then be needed to meet the specification on velocity.

Conclusions

1. A promising form of hybrid navigation is to update an inertial navigator at intervals less than one tenth the Schuler period, because the error build-up during this interval is very small in comparison to the long-term drift which is normally used as the figure of merit.

2. Error growth in the inertial navigator during this interval is well approximated by straight integrations.
3. Accelerometer noise has the greater effect on the error of an aligned system for $t < \frac{3.0}{\gamma\omega_s}$. Gyro drift predominates after that time.
4. For continuous filtering, the accelerometer error predominates for $\gamma\omega_s < \omega_n$.
5. Filter performance for cases of practical interest can be predicted on the basis of simple, analytic models. These same models can be used to design the filter.
6. It is not necessary to estimate the platform misalignment as long as there is continuous external position data. Even though the angles get large, the filter is continually estimating the velocity error which they produce. The main reason for estimating misalignment angles is to be able to navigate accurately in the event the external position information is lost.
7. Position accuracy is most strongly influenced by the external position fix accuracy. Velocity accuracy is most strongly influenced by accelerometer noise.

8. For update times which are shorter than $1/\omega_n$ and one tenth Schuler period, the discrete filter performance can be predicted by the analytic results of the continuous case.

REFERENCES

1. Britting, K.R., "State Transition Matrix for Inertial Navigation Systems," M.I.T. Experimental Astronomy Lab Report RE-53, March, 1969.
2. Dushman, Allan, "On Gyro Drift Models and their Evaluation," I.R.E. Transactions on Aerospace and Navigational Electronics, December, 1962.
3. Brock, L.D., "Application of Statistical Estimation Techniques to Navigation Systems," M.I.T. Ph.D. Thesis, June, 1965.
4. Kalman, R.E., and Bucy, R.S., "New Results in Linear Filtering and Prediction Theory," Transactions of the ASME, Journal of Basic Engineering, March, 1961.
5. Madigan, R.J., and Koenke, E.J., "Aided Inertial Flight Test Experiments," AGARD Guidance and Control Panel Symposium, Cambridge, Massachusetts, May, 1969.
6. Potter, J.E., and VanderVelde, W.E., "Optimum Mixing of Gyroscope and Star Tracker Data," M.I.T. Experimental Astronomy Lab Report RE-26, February, 1967.
7. Brayard, M.C., "Optimum Mixing of Inertial Navigator Data and Radar Data," M.I.T. S.M. Thesis, June, 1969.

New Technology Appendix

After a diligent review of the work performed under this contract, no new innovation, discovery, improvement or invention was made."